

Palmitoylation of CCR5 Is Critical for Receptor Trafficking and Efficient Activation of Intracellular Signaling Pathways*

Received for publication, January 21, 2001, and in revised form, April 20, 2001
Published, JBC Papers in Press, April 25, 2001, DOI 10.1074/jbc.M100583200

Cédric Blanpain,^{a,b,c} Valérie Wittamer,^{a,b,d} Jean-Marie Vanderwinden,^{a,e}
Alain Boom,^f Benoît Renneboog,^{a,c} Benhur Lee,^{g,h} Emmanuel Le Poul,ⁱ Laïla El Asmar,^a
Cédric Govaerts,^{a,j} Gilbert Vassart,^{a,k} Robert W. Doms,^{g,l} and Marc Parmentier^{a,m}

From the ^aInstitute of Interdisciplinary Research, ^dLaboratoire de Neurophysiologie, ^fLaboratoire d'Histologie de Neuroanatomie et de Neuropathologie, and ^kService de Génétique Médicale, Université Libre de Bruxelles, Campus Erasme, 808 Route de Lennik, B-1070 Brussels, Belgium, the ^gDepartment of Pathology and Laboratory Medicine, University of Pennsylvania, Philadelphia, Pennsylvania 19104, and ^lEuroscreen S.A. 802 Route de Lennik, B-1070 Brussels, Belgium

CCR5 is a CC chemokine receptor expressed on memory lymphocytes, macrophages, and dendritic cells and also constitutes the main coreceptor for macrophage-tropic (or R5) strains of human immunodeficiency viruses. In the present study, we investigated whether CCR5 was palmitoylated in its carboxyl-terminal domain by generating alanine substitution mutants for the three cysteine residues present in this region, individually or in combination. We found that wild-type CCR5 was palmitoylated, but a mutant lacking all three Cys residues was not. Through the use of green fluorescent fusion proteins and immunofluorescence studies, we found that the absence of receptor palmitoylation resulted in sequestration of CCR5 in intracellular biosynthetic compartments. By using the fluorescence recovery after photobleaching technique, we showed that the non-palmitoylated mutant had impaired diffusion properties within the endoplasmic reticulum. We next studied the ability of the mutants to bind and signal in response to chemokines. Chemokines binding and activation of G_i-mediated signaling pathways, such as calcium mobilization and inhibition of adenylate cyclase, were not affected. However, the duration of the

functional response, as measured by a microphysiometer, and the ability to increase [³⁵S]guanosine 5'-3-O-(thio)triphosphate binding to membranes were severely affected for the non-palmitoylated mutant. The ability of RANTES (regulated on activation normal T cell expressed and secreted) and aminooxypentane-RANTES to promote CCR5 endocytosis was not altered by cysteine replacements. Finally, we found that the absence of receptor palmitoylation reduced the human immunodeficiency viruses coreceptor function of CCR5, but this effect was secondary to the reduction in surface expression. In conclusion, we found that palmitoylated cysteines play an important role in the intracellular trafficking of CCR5 and are likely necessary for efficient coupling of the receptor to part of its repertoire of signaling cascades.

CCR5 is a high affinity receptor for the CC chemokines MIP-1 α , MIP-1 β , RANTES¹ (1), MCP-2 (2), LD78 β (3), and a proteolytically processed variant of HCC-1 (HCC-1-(9–78)) (4). It is also the principal coreceptor for macrophage-tropic strains of HIV (5, 6). HIV-1 infection is initiated by the interaction of the virion envelope glycoprotein with cellular CD4 and a coreceptor that belongs to the G protein-coupled receptor (GPCR) family. CCR5-using (R5) strains predominate during the early stages of the disease and are responsible for viral transmission. The major role of CCR5 in AIDS pathogenesis has been demonstrated by the almost complete resistance to HIV-1 infection of individuals homozygous for a 32-base pair deletion (Δ 32 allele) in the coding region of the receptor (7, 8). A prominent role of CCR5 has also been suggested in the recruitment of leukocyte populations in other human diseases, such as rheumatoid arthritis, multiple sclerosis, and asthma (9–13).

CCR5 surface expression can be regulated at multiple levels. Repression of *CCR5* gene transcription has been achieved in T cells by CD28 engagement (14). Sequestration of mutated re-

* This work was supported in part by the Actions de Recherche Concertées de la Communauté Française de Belgique, the French Agence Nationale de Recherche sur le SIDA, the Center de Recherche Inter-universitaire en Vaccinologie, the Belgian program on interuniversity poles of attraction initiated by the Belgian State, Prime Minister's Office, Science Policy Programming, the BIOMED and BIOTECH program of the European Community Grants BIO4-CT98-0543 and BMH4-CT98-2343, the Fonds de la Recherche Scientifique Médicale of Belgium, Télévie, the Fondation Médicale Reine Elisabeth (to M. P.), by National Institutes of Health Grant R01 40880, a grant from the Burroughs Wellcome Fund (to R. W. D.), and by National Institutes of Health Grant K08 HL03923 (to B. H. L.). The costs of publication of this article were defrayed in part by the payment of page charges. This article must therefore be hereby marked "advertisement" in accordance with 18 U.S.C. Section 1734 solely to indicate this fact.

^b Both authors contributed equally to this work.

^c Aspirant of the Belgian Fonds National de la Recherche Scientifique.

^d Recipient of a First Fellowship of the Région Wallonne.

^e Chercheur Qualifié of the Belgian Fonds National de la Recherche Scientifique.

^h Recipient of the Burroughs Wellcome Fund Career Development award.

^j Recipient of a fellowship of the Fonds pour la Recherche dans l'Industrie et l'Agriculture.

^l Recipient of an Elizabeth Glaser Scientist Award.

^m To whom correspondence should be addressed: IRIBHN, ULB Campus Erasme, 808 Route de Lennik, B-1070 Brussels, Belgium. Tel.: 32-2-5554171; Fax: 32-2-5554655; E-mail: mparmentier@ulb.ac.be.

¹ The abbreviations used are: RANTES, regulated on activation normal T cell expressed and secreted; AOP, aminooxypentane; HIV, human immunodeficiency virus; BSA, bovine serum albumin; CHO, Chinese hamster ovary; DMEM, Dulbecco's modified Eagle's medium; ER, endoplasmic reticulum; FRAP, fluorescence recovery after photobleaching; GFP, green fluorescent protein; GPCR, G protein-coupled receptor; KRH, Krebs-Ringer HEPES; mAb, monoclonal antibody; MCF, mean channel fluorescence; PAGE, polyacrylamide gel electrophoresis; PBS, phosphate-buffered saline; PE, phycoerythrin; RGS, regulator of G protein signaling; Tris-buffered saline; wt, wild-type; GTP γ S, guanosine 5'-3-O-(thio)triphosphate; FACS, fluorescence-activated cell sorter; PTX, pertussis toxin.

ceptors in the endoplasmic reticulum (ER) has been described for the $\Delta 32$ variant and for other CCR5 variants known to affect chemokine receptor or coreceptor functions (15, 16). The level of CCR5 at the cell surface is also regulated by endocytosis, and this mechanism contributes to the blocking of HIV entry by chemokines and chemokine analogs (17–19). Several post-translational modifications have also been shown to influence CCR5 expression. Activation of CCR5 by chemokines induces phosphorylation of serine residues within the carboxyl-terminal domain, and this, in turn, plays an important role in receptor desensitization and internalization (20). Two disulfide bonds linking CCR5 extracellular domains are necessary for maintaining a structural conformation of the receptor compatible with efficient trafficking to the cell surface, ligand binding, and induction of intracellular signaling (21). Sulfation of CCR5 amino-terminal tyrosines has also been shown to play an important role in gp120 binding and HIV entry (22).

It is well established that for some GPCRs, such as the β_2 -adrenergic receptor, palmitoylation of cysteine residues in their cytoplasmic tails can modulate their biological activities (23). It has been suggested that this acylation provides a membrane anchor to the carboxyl-terminal domain and creates a fourth intracellular loop. Palmitate is bound to cysteine side chains through a reversible thioester bond and increases the overall hydrophobicity of the protein domain. Palmitoylation of GPCRs has been shown to affect different functions of the receptors, such as membrane targeting, signaling properties, endocytosis, and recycling. Because of the pleiotropic effects of palmitoylation that have been described on the function of various receptor families (23), it is not possible to predict how palmitoylation will affect a specific receptor. No information concerning palmitoylation and its role in chemokine receptors has been reported so far. Most, but not all, chemokine receptors display cysteines in their carboxyl-terminal tails, at positions compatible with palmitoylation. CCR5 has a cluster of three cysteines in this region (Fig. 1A). In the present study, we investigated the role played by these three cysteine residues in various aspects of CCR5 function. We provide evidence that CCR5 is indeed palmitoylated on these residues. We also found that palmitoylation is necessary to allow efficient CCR5 trafficking to the cell surface and for efficient triggering of intracellular signal transduction pathways.

MATERIALS AND METHODS

Mutagenesis and CCR5 Constructs—The three cysteines located within the carboxyl-terminal domain of CCR5 (Cys-321, Cys-323, and Cys-324) were mutated into alanine, individually or in combination, by site-directed mutagenesis using the Quickchange method (Stratagene). The 3CysA mutant refers to a receptor in which all three cysteines have been mutated to alanine. Alanine substitutions were made instead of more conservative serine substitutions, in order to avoid additional phosphorylation of the receptor tail. Following sequencing of the constructs, the mutated reading frames were subcloned into the bicistronic expression vector pEFIN3 as described previously (24) for generation of stable cell lines and in pcDNA3 (Invitrogen) for the HIV-1 infection assay. All constructs were verified by sequencing before transfection. Constructs encoding fusion proteins between wtCCR5, or the 3CysA mutant, and enhanced GFP (Packard Instrument Co.) linked to the carboxyl terminus of CCR5 were generated by PCR. CCR5 was amplified with a forward primer containing a *Bam*HI restriction site (5'-TCGAGGATCCAAGATGGATTATCAAGTGTC-3') and a reverse primer replacing the TGA stop codon by an *Xho*I restriction site (5'-TCGACTCGAGCAAGCCACAGATATTTCC-3'). Enhanced GFP was amplified by a forward primer containing an *Xho*I restriction site, followed by a flexible tri-glycine linker replacing the ATG start codon (5'-TCGACTCGAGGGGGGAGGTGTGAGCAAGGGCGAGGAG-3') and a reverse primer containing an *Xba*I restriction site after the stop codon (5'-TCGATCTAGATTACTTGTACAGCTCGTCC-3'). Enhanced GFP was then cloned in frame with the CCR5 carboxyl terminus using the *Xho*I restriction site and the linker sequence LEGGG between the two coding regions. After checking the constructs by sequencing, the fusion

proteins coding sequences were transferred into the bicistronic vector pEFIN3, using the *Bam*HI and *Xba*I restriction sites.

Expression of Mutant Receptors in CHO-K1 Cell Lines—CHO-K1 cells were cultured using Ham's F-12 medium supplemented with 10% fetal calf serum (Life Technologies, Inc.), 100 units/ml penicillin, and 100 μ g/ml streptomycin (Life Technologies, Inc.). A plasmid encoding apoaequorin under control of the SR α promoter (25) was transfected into CHO-K1 cells, using Fugene 6 (Roche Molecular Biochemicals). Puromycin (100 μ g/ml, Calbiochem) selection of transfectants was initiated 2 days after transfection. Individual clones were isolated 3 weeks later, and the most responding clone was selected on the basis of its functional response (luminescence signal) to ionomycin A (100 nM) and ATP (10 μ M). Constructs encoding wild-type CCR5 and the various cysteine mutants in the pEFIN3 bicistronic vector were further transfected using Fugene 6 in this apoaequorin-expressing cell line. Selection of transfected cells was made for 14 days with 400 μ g/ml G418 (Life Technologies, Inc.), and the population of mixed cell clones expressing wild-type or mutant receptors was used for binding and functional studies. Clones expressing similar amounts of wtCCR5 or 3CysA at the cell surface were selected (clones CCR5-c3 and 3CysA-c1 respectively) following establishment of clonal cell lines by limit dilution and screening by FACS analysis. Clonal CHO-K1 cell lines stably expressing the fusion proteins wtCCR5-GFP and 3CysA-GFP were also established and selected by fluorescence microscopy.

[³H]Palmitic Acid Incorporation—Mixed cell populations expressing wtCCR5 or the various cysteine mutants, as well as the clonal lines CCR5-c3 and 3CysA-c1, were assayed for [³H]palmitic acid incorporation. Approximately 5×10^6 cells, at 70% confluence in 10-cm dishes, were washed twice with cold PBS and incubated for 18 h in serum-free Ham's F-12 medium. Cells were washed once with cold phosphate-buffered saline (PBS, pH 7.4) and metabolically labeled with 0.2 mCi/ml [9,10-³H]palmitic acid (Amersham Pharmacia Biotech) for 4 h at 37 °C. The incubation was stopped by washing the cells twice with cold PBS, and the cells were solubilized in 1 ml of solubilization buffer (10 mM Tris-HCl, pH 7.4, containing 100 mM NaCl, 2 mM EDTA, 1 tablet of Protease Inhibitor Mixture (Roche Molecular Biochemicals) per 10 ml, and 1% (w/v) Cymal TM5 (Antrace, Maumee, OH)) as described (26) for 1 h at 4 °C under constant agitation, and cell debris was removed by ultracentrifugation for 30 min at $45,000 \times g$ and 4 °C. Solubilized receptors were incubated overnight at 4 °C with 10 μ g/ml 2D7, a mAb recognizing a conformation epitope in the second extracellular loop of CCR5, then immunoprecipitated by protein G-Sepharose (Amersham Pharmacia Biotech) for 2 h at 4 °C, and washed three times in solubilization buffer. Samples were resuspended in SDS-PAGE sample buffer, heated for 1 h at 55 °C, and separated onto 12% gels. One SDS-PAGE, performed with 20% of the immunoprecipitated samples, was transferred to nitrocellulose filters. The filters were incubated, for CCR5 immunodetection, with MC5 (0.5 μ g/ml), a monoclonal antibody recognizing a linear epitope in CCR5 amino terminus, and then with a horseradish peroxidase-coupled goat anti-mouse antibody, and the immunoblot was revealed by enhanced chemiluminescence (Amersham Pharmacia Biotech). The SDS-PAGE performed with the remaining samples was incubated in the Amplify fluorographic reagent (Amersham Pharmacia Biotech) and dried, and autofluorography was performed for 3 weeks at -70 °C with x-ray films (Fuji).

FACS Analysis—Cell surface expression of the CCR5 variants was measured by flow cytometry using phycoerythrin-conjugated 2D7 (Becton Dickinson), or MC-5. FACS analysis was performed on a FACScan flow cytometer using the CellQuest software (Becton Dickinson). The mean channel fluorescence (MCF) was used to compare the levels of receptor expression at the cell surface. Results were normalized for the MCF obtained for wtCCR5 with the 2D7 antibody (100%) after subtraction of the nonspecific fluorescence obtained for untransfected cells (0%).

Confocal Microscopy—For immunofluorescence studies, stable CHO-K1 cell lines expressing wild-type or mutant CCR5 were grown on uncoated glass coverslips for 24 h. Coverslips were rinsed with PBS, fixed for 10 min in 3% paraformaldehyde in PBS, and washed three times for 10 min with Tris-buffered saline (TBS). For intracellular staining, the cells were permeabilized by a 5-min incubation with 0.15% Triton X-100 in TBS and washed three times in TBS. Fixed or permeabilized cells were incubated for 1 h at room temperature with 5% normal sheep serum in TBS. Incubation with 5 μ g/ml of the MC-5 mAb was performed overnight in the presence of 5% normal sheep serum. Cells were rinsed three times in TBS, incubated for 60 min in the dark with a fluorescein isothiocyanate-labeled sheep anti-mouse IgG antibody (1:30 dilution, Amersham Pharmacia Biotech), washed three times in TBS and once in water, and mounted with a drop of gelvatol solution

containing 100 mg/ml 1,4-diazabicyclo(2.2.2)octane antifading agent (Sigma). Cells were observed on an MRC 1024 confocal microscope (Bio-Rad) fitted on an Axiovert 100 inverted microscope (Zeiss, Oberkochen, Germany) equipped with a Plan-NeofluarTM 40×/1.3 oil immersion objective (Zeiss). The 488 nm excitation beam of an argon-krypton laser and a 522/32 nm band-pass emission filter were used for selective viewing of the green fluorochrome. Fields of interest (512 × 512 pixels) were selected visually. The gray scale data sets generated were transferred to an IndyTM work station (Silicon Graphics, Mountain View, CA) running the ImageSpaceTM software (Molecular Dynamics, Sunnydale, CA). No labeling was observed on untransfected CHO-K1 cells using MC-5 or on transfected cells using a control IgG mAb (data not shown). Figures were prepared on a PowerMacTM (Apple, Cupertino, CA) running FreehandTM (Macromedia, San Francisco, CA) and IllustratorTM (Adobe, San Francisco, CA) software.

For the confocal study of wtCCR5-GFP or 3CysA-GFP in living cells, the cell clones were seeded the day before the analysis on 22-mm round glass coverslips and grown for 18 h in a CO₂ incubator. Cells were rinsed in DMEM/F-12 (Life Technologies, Inc.), and the coverslips were placed in a 1-ml chamber with 200 μl of culture medium. Experiments were performed at 37 °C on a temperature-controlled stage, and images were analyzed as described above for immunofluorescence studies.

FRAP Analysis of wtCCR5-GFP and 3CysA-GFP Fusion Proteins in Living Cells—Diffusion of the receptor within the intracellular cell membrane compartments was measured by fluorescence recovery after photobleaching (FRAP) using the MRC 1024 confocal microscope (see above). A defined region was photobleached at full laser power (100%) for 10 scans, and recovery was monitored by scanning the whole cell at low laser power (3 to 10%). The first image was recorded 30–40 s after photobleaching (the time required for adjusting the optics and resetting the instrument), and subsequent images were recorded every 20 s. Quantitative measurements of fluorescence, for generating recovery plots, and *D* and *M* values, were obtained by using macros written in the NIH Image freeware. The fluorescence signal of an unbleached cell area was measured before and at each time point after photobleaching. All FRAP values were normalized according to these control values, but even after 60 scans, the correction factor never exceeded 20% of the initial value. Diffusion parameters were obtained as described (27) and were calculated by non-linear regression using the GraphPad PRISM software.

Binding Assays—Mixed populations of CHO-K1 cells expressing wild-type or mutant CCR5 were collected from plates with Ca²⁺- and Mg²⁺-free PBS supplemented with 5 mM EDTA, gently pelleted for 2 min at 1000 × *g*, and resuspended in binding buffer (50 mM HEPES, pH 7.4, 1 mM CaCl₂, 5 mM MgCl₂, 0.5% BSA). Competition binding assays were performed in Minisorb tubes (Nunc, Roskilde, Denmark), using 0.08 nM [¹²⁵I]-MIP-1β (2200 Ci/mmol, PerkinElmer Life Sciences) as tracer for wtCCR5 and the single cysteine mutant or 0.12 nM [¹²⁵I]-MIP-1β for the double and triple cysteine mutants, variable concentrations of competitors, and 40,000 cells in a final volume of 0.1 ml. Total binding was measured in the absence of competitor, and nonspecific binding was measured in the presence of a 100-fold excess of unlabeled ligand. Samples were incubated for 90 min at 27 °C and then bound tracer was separated by filtration through GF/B filters presoaked in 1% BSA. Filters were counted in a β-scintillation counter. Binding parameters were determined with the PRISM software (Graphpad Software, San Diego, CA) using nonlinear regression applied to a one-site competition model.

Aequorin-based Functional Assay—The functional response to chemokines was analyzed by measuring the luminescence of aequorin as described (21, 28). Cells were collected from plates with Ca²⁺- and Mg²⁺-free PBS supplemented with 5 mM EDTA, pelleted for 2 min at 1000 × *g*, resuspended in DMEM at a density of 5 × 10⁶ cells/ml, and incubated for 2 h in the dark in the presence of 5 μM coelenterazine H (Molecular Probes, Eugene, OR). Cells were diluted 7.5-fold before use. Agonists in a volume of 50 μl of DMEM were added to 50 μl of the cell suspension (33,000 cells), and luminescence was measured for 30 s in a EG & G Berthold (PerkinElmer Life Sciences). Functional parameters were determined with the PRISM software (Graphpad Software) using nonlinear regression applied to a sigmoidal dose-response model.

Inhibition of cAMP Accumulation—CCR5-c3 and 3CysA-c1 cells were spread on Petri dishes (250,000 cells per 35-mm dish) and cultured overnight in Ham's F-12 medium containing 10% fetal calf serum, 100 units/ml penicillin, 100 μg/ml streptomycin, and 400 μg/ml G418. Cells were preincubated for 30 min in Krebs-Ringer HEPES (KRH) buffer composed of 25 mM HEPES, pH 7.4, 124 mM NaCl, 5 mM KCl, 1.25 mM MgSO₄, 1.45 mM CaCl₂, 1.25 mM KH₂PO₄ and 8 mM glucose and then incubated for 15 min in the same medium supplemented with 10 μM

forskolin and variable concentrations of MIP-1β. The cAMP accumulation was stopped by replacing the medium with 0.1 M HCl. Cells debris were pelleted by centrifugation at 14,000 rpm for 10 min, and the supernatant was dried off in a vacuum concentrator. The cAMP levels were measured by a radioimmunoassay kit (TRK 432, Amersham Pharmacia Biotech) according to the procedure specified by the manufacturer. The basal cAMP level was determined in the absence of forskolin stimulation and subtracted from forskolin-stimulated values. Functional parameters were determined with the PRISM software (Graphpad Software), using nonlinear regression. The data represent the inhibition of forskolin-stimulated cAMP accumulation, and the experiments were performed in duplicate.

Microphysiometry—CCR5-c3 or 3CysA-c1 cells were plated onto the membrane of Transwell capsules (Molecular Devices), at a density of 2.5 × 10⁵ cells/well in Ham's F-12 medium. The next day, the capsules were transferred to a microphysiometer (Cytosensor, Molecular Devices), and the cells were allowed to equilibrate for ~2 h by perfusion of 1 mM phosphate-buffered RPMI 1640 medium (pH 7.4). Cells were then exposed to MIP-1β at the final concentration of 100 nM for 2 min. Acidification rates were measured at 1-min intervals.

GTPγS Binding Assay—For the measurement of RANTES-stimulated GTPγS binding to membranes of cells expressing wtCCR5 or the 3CysA mutant, membranes (10 or 20 μg) from CCR5-c3 or 3CysA-c1 cells were incubated for 15 min at room temperature in GTPγS binding buffer (20 mM HEPES, pH 7.4, 100 mM NaCl, 3 mM MgCl₂, 3 μM GDP, 10 μg/ml saponin) containing different concentrations of RANTES, in 96-well microplates (Basic FlashPlates, PerkinElmer Life Sciences). [³⁵S]GTPγS (0.1 nM, Amersham Pharmacia Biotech) was added, and microplates were shaken for 1 min and further incubated at 30 °C for 30 min. The incubation was stopped by centrifugation of the microplate for 10 min, at 800 × *g* and at 4 °C, and aspiration of the supernatant. Microplates were counted in a TopCount (Packard Instrument Co.) for 1 min per well. Functional parameters were determined with the PRISM software (Graphpad Software) using non-linear regression applied to a sigmoidal dose-response model.

Endocytosis Assay—Chemokine-induced CCR5 endocytosis was quantified as described (19). Briefly, CCR5-c3 or 3CysA-c1 cells were collected from plates with 5 mM EDTA in PBS, washed with DMEM/F-12, and incubated for 45 min at 37 °C with RANTES or AOP-RANTES at different concentrations. Cells were washed twice with 3 ml of cold PBS supplemented with 0.1% sodium azide and 0.1% BSA, and incubated for 30 min at 4 °C with MC-5 (a monoclonal antibody that does not compete with RANTES binding), then stained with a phycoerythrin-conjugated anti-mouse Ig antibody (Sigma). Cells were further washed and resuspended, and their cell fluorescence was analyzed by FACS.

HIV-1 Infection Assay—GFP was cloned in place of the luciferase gene in the pNL-R-E-luc plasmid (29), and GFP reporter viruses were created by cotransfecting the pNL-R-E-GFP plasmid with plasmids encoding the appropriate Env protein. GFP reporter viruses were used in infection assays in a similar manner to luciferase reporter viruses (29). Target cells were prepared by cotransfecting 293T cells with a CD4 plasmid and a variable amount of coreceptor-encoding plasmid. Incubation was done at 37 °C. Two days post-infection, cells were stained for 30 min with the phycoerythrin-labeled 2D7 mAb, washed, fixed with 3% paraformaldehyde, and cell fluorescence was analyzed by FACS, using a FACScan flow cytometer and the CellQuest software (Becton Dickinson, San Jose, CA). pcDNA3-transfected cells infected with the same amount of GFP reporter viruses were used as controls for background GFP expression. The MCF was used to compare the levels of receptor expression at the cell surface. HIV infection was determined by counting GFP-positive and dual-positive (GFP+2D7-PE) cells.

RESULTS

Palmitoylation is known to occur on cysteine residues located in the carboxyl-terminal domain of GPCRs. It has been associated with the modulation of various functional properties, depending on the specific receptor (23). CCR5 exhibits a cluster of 3 cysteines in its carboxyl-terminal domain (Cys-321, Cys-323, and Cys-324) (Fig. 1, *A* and *B*), suggesting that it could be palmitoylated. In order to test the role of these intracellular cysteines on CCR5 function, we mutated these 3 residues into alanine, individually (mutants C321A, C323A, and C324A) or in all possible combinations (C321A/C323A, C321A/C324A, C323A/C324A, 3CysA = C321A/C323A/C324A). The various constructs were inserted into efficient bicistronic vectors and transfected in CHO-K1 cells stably expressing the reporter

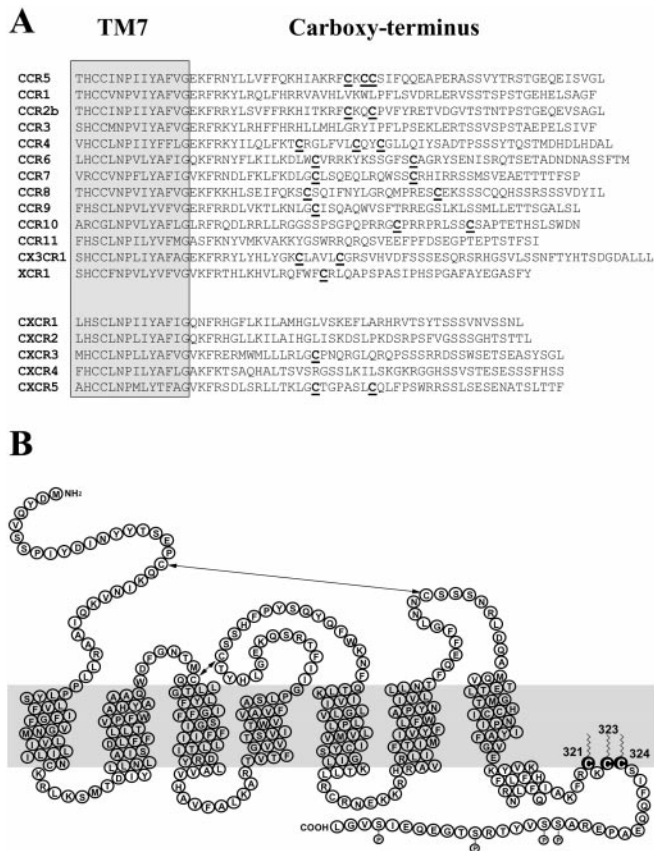


FIG. 1. Primary sequence of the carboxyl-terminal tail of human chemokine receptors and schematic representation of CCR5. *A*, alignment of the carboxyl-terminal tail of chemokine receptors. Cysteine residues are highlighted in **bold** and underlined, and the seventh transmembrane domain is boxed. *B*, the putative palmitoylation organization of CCR5 is represented, and the potential palmitoylation sites Cys-321, Cys-323, and Cys-324 are indicated in black.

protein apoaequorin. Mixed populations of transfected cells were used for testing surface expression, binding, and functional properties of the receptors. We also selected clonal cell lines expressing wtCCR5 and the 3CysA mutant at similar levels (respectively clones CCR5-c3 and 3CysA-c1) and performed the various assays as well.

CCR5 Is Palmitoylated and Mutation of the Cysteine Cluster in Its Carboxyl-terminal Domain Abrogates [³H]Palmitic Acid Incorporation—Mixed CHO-K1 cells expressing wtCCR5 or the various mutants, as well as the CCR5-c3 and 3CysA-c1 clones, were incubated with [³H]palmitate. Following cell lysis, the receptor was immunoprecipitated and subjected to SDS-PAGE followed by autoradiography. A fraction of the immunoprecipitate was migrated separately and blotted onto a nitrocellulose membrane, and the receptor was detected by immunochrometry. Variable amounts of mature receptor (43 kDa) were detected for the different mutants (Fig. 2A), in accordance to the FACS data (see below). Similar amounts were detected for the CCR5-c3 and 3CysA-c1 clones. wtCCR5 and single cysteine mutants incorporated [³H]palmitate much more efficiently than mutants containing one or no cysteine (3CysA). No significant differences were observed among the single cysteine mutants, demonstrating that the three cysteines play equivalent roles and that the cluster represents the major site of CCR5 palmitoylation (Fig. 2B).

All Three Cysteines Contribute to the Efficient Export of CCR5 to the Plasma Membrane—Pools of transfected CHO-K1 cells were assayed for cell surface expression by FACS analysis using the conformation-sensitive 2D7 mAb (30). As shown in

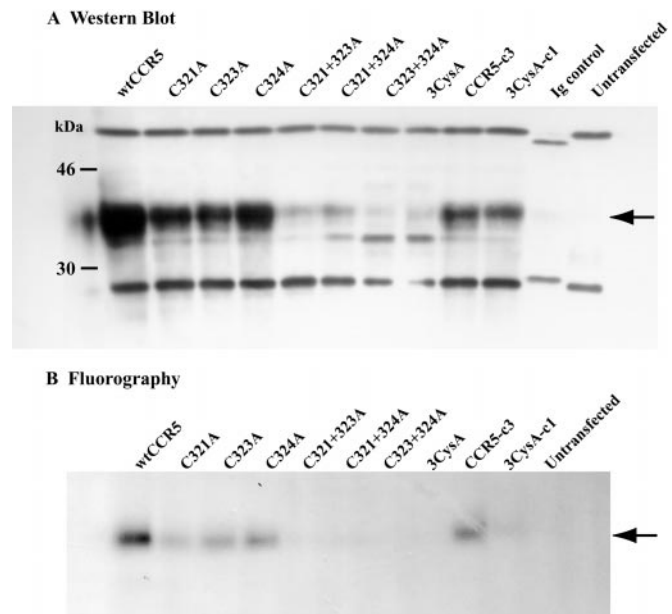


FIG. 2. Incorporation of [³H]palmitate into wild-type and mutant CCR5. Mixed CHO-K1 cells expressing wtCCR5 or the various mutants, as well as the CCR5-c3 and 3CysA-c1 clones, were metabolically labeled for 4 h with [³H]palmitic acid. The receptor was immunoprecipitated from cell lysates by the anti-CCR5 mAb 2D7. Immune complexes were separated by SDS-PAGE. CCR5 was either immunodetected following Western blotting of the samples using mAb MC-5 (*A*) or the gel was subjected to fluorography and autoradiography (*B*). Controls included immunoprecipitation using wtCCR5-expressing cells and an isotype (IgG1) of the 2D7 monoclonal (Ig control) and immunoprecipitation using untransfected CHO-K1 cells and the 2D7 monoclonal antibody (untransfected). The Western blot and fluorography shown are representative of two independent experiments.

Fig. 3, *A* and *B*, the mutation of any one of the three cysteines (mutants C321A, C323A, and C324A) reduced cell surface expression by 50%. No significant difference was seen between the three mutants. The double mutants (C321A/C323A, C321A/C324A, and C323A/C324A) and to a larger extent the triple mutant (3CysA) showed even greater decreases in surface expression. This gradual decrease in cell surface expression, according to the number of substituted cysteines, was also seen with MC-5, a mAb recognizing a linear epitope, suggesting a reduction in the number of receptors at the plasma membrane rather than an alteration of the receptor conformation. Surface expression of the selected clones CCR5-c3 and 3CysA-c1 is illustrated for comparison (Fig. 3C).

To investigate the relative role of decreased protein synthesis and export impairment, the subcellular distribution of receptor immunoreactivity was analyzed by confocal microscopy, using the MC-5 mAb. In the absence of permeabilization, strong staining was obtained for most cells of the mixed population expressing wtCCR5 but was markedly reduced for the 3CysA mutant and restricted to a small fraction of the cell population (Fig. 4A). When cells were permeabilized, strong intracellular staining could be seen in most cells of both wtCCR5 and the 3CysA mutant (Fig. 4B). The presence of strong perinuclear staining in 3CysA-expressing cells suggested that the mutant receptor is synthesized efficiently but sequestered in the endoplasmic reticulum and/or the Golgi complex where palmitoylation might take place (31).

CCR5 Palmitoylation Increases Its Diffusion Rate in Intracellular Compartments—The dynamics of fusion proteins between wtCCR5 or 3CysA and GFP were analyzed by confocal microscopy in clonal cell lines. wtCCR5-GFP was detected at the plasma membrane, although a fraction of the receptor was also seen intracellularly. The 3CysA-GFP mutant was mainly

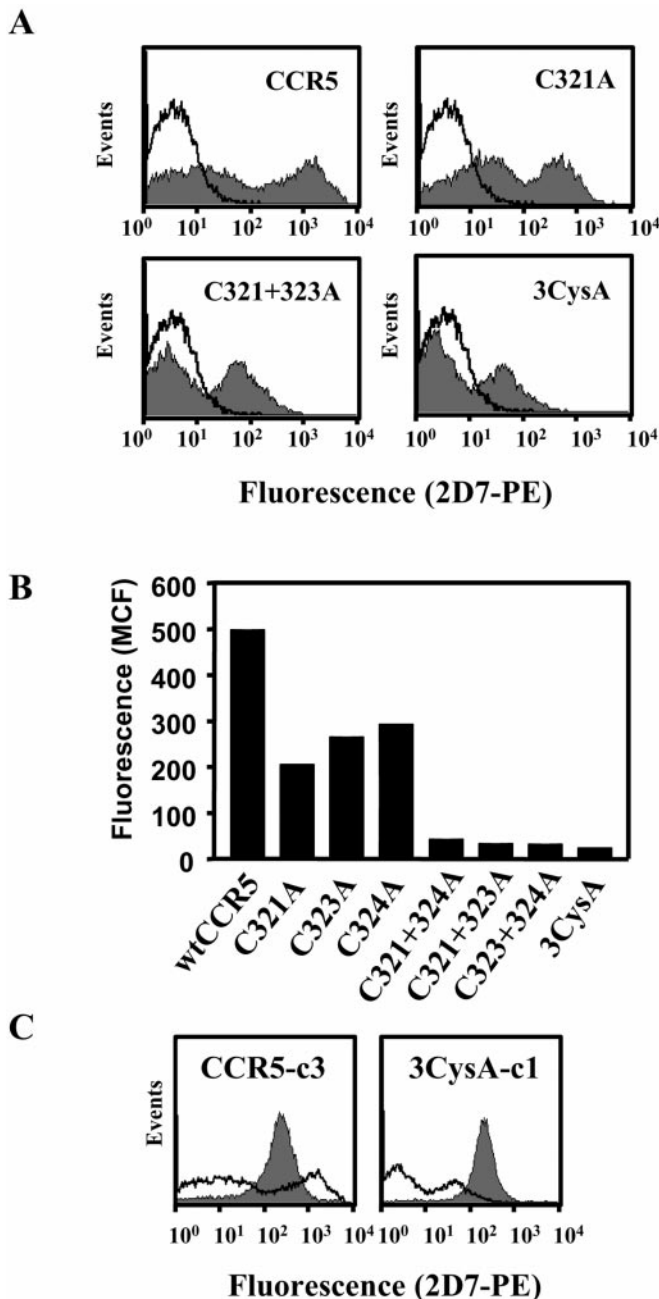


FIG. 3. Surface expression of CCR5 mutants in populations of transfected cells. *A*, cell surface expression of wtCCR5 and selected cysteine mutants in pools of transfected CHO-K1 cells, as analyzed by FACS using phycoerythrin-conjugated 2D7, a mAb mapping to the second extracellular loop of the receptor. The displayed patterns are representative of the various combinations of cysteine mutations. The fluorescence of untransfected cells stained with 2D7 is overlaid in each panel. *B*, MCF obtained for all mutants expressed in CHO-K1 cells, using the 2D7 mAb. A typical experiment out of the three performed independently is represented. *C*, cell surface expression of the receptor in clones stably expressing wtCCR5 (CCR5-c3) or the 3CysA mutant (3CysA-c1), as analyzed by FACS, using the PE-labeled 2D7 mAb. The fluorescence of the population of transfected cells from which the individual clones were isolated is overlaid in each panel.

localized intracellularly (Fig. 4C). The ability of wtCCR5-GFP and the 3CysA-GFP mutant to diffuse within intracellular compartments was quantified using the FRAP technique (32), in which the fluorescent protein present in a small area is irreversibly photobleached by an intense laser flash. The fluorescence recovery through exchange of bleached and non-bleached protein was measured every 20 s using an attenuated laser

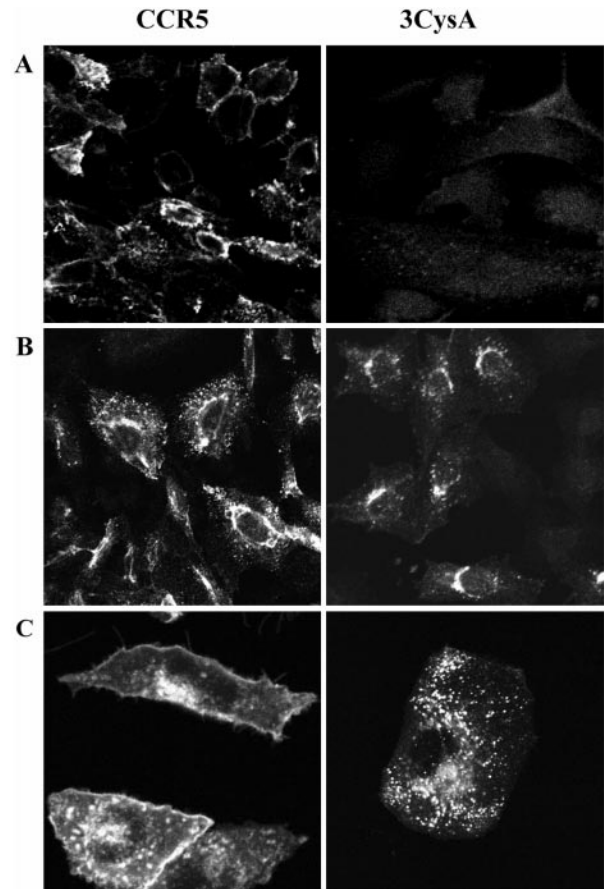


FIG. 4. Subcellular distribution of CCR5 and the 3CysA mutant. *A* and *B*, subcellular distribution of wtCCR5 and 3CysA, as analyzed by confocal microscopy using MC-5, a mAb recognizing a linear epitope on the receptor amino terminus. Paraformaldehyde-fixed cells were permeabilized (*B*) or not (*A*) with 0.15% Triton X-100 before staining. The figures shown are representative of two independent experiments. *C*, subcellular distribution of wtCCR5-GFP and 3CysA-GFP fusion proteins, as analyzed by confocal microscopy.

beam (not shown). Quantitative FRAP analysis showed that fluorescence recovery was more rapid and more complete for wtCCR5-GFP, with a diffusion constant of $1.47 \cdot 10^{-9} \text{ cm}^2/\text{s}$ and a mobile fraction of 100%, whereas the 3CysA-GFP mutant was characterized by a diffusion constant of $0.43 \cdot 10^{-9} \text{ cm}^2/\text{s}$ with a mobile fraction of only 60% (Fig. 5), suggesting that palmitoylation of CCR5 increases its mobility in intracellular membrane compartments.

Role of CCR5 Palmitoylation in G Protein Coupling and Intracellular Signaling—The binding parameters (B_{max} and K_i) of mixed cell populations expressing the various mutants were determined by a homologous competition binding assay, using ^{125}I -MIP-1 β as tracer. A reduction in the number of binding sites (calculated B_{max}) was observed for all mutants, particularly when more than one cysteine was substituted, in full agreement with the results of the FACS analysis. The affinity of the cysteine mutants for MIP-1 β did not change significantly, however, as compared with wtCCR5, with K_i values ranging from 0.2 to 0.7 nM (Fig. 6A and Table I).

We next tested the ability of these non-clonal cell populations expressing the various cysteine mutants to trigger intracellular calcium release, using the aequorin assay. As shown in Fig. 6B, mutation of a single cysteine resulted in a moderate reduction of the efficacy of calcium signaling in response to MIP-1 β (50% of wtCCR5) but with a similar potency (Table I). The functional responses of the double and triple mutants were more severely affected, as no signal was obtained in response to the highest

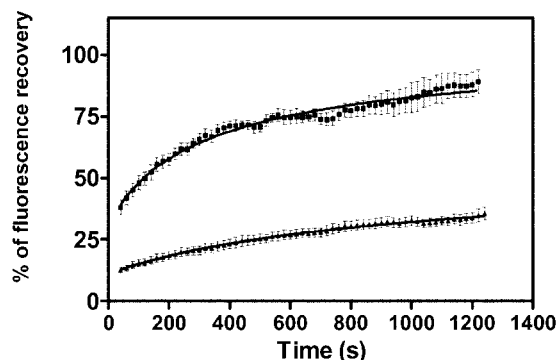


FIG. 5. FRAP of wtCCR5-GFP and 3CysA-GFP in ER membranes. Quantitative time course of fluorescence recovery for wtCCR5-GFP and 3CysA-GFP in the ER. Measurements were taken every 20 s. The displayed curves represent the mean and S.E. of at least five independent measurements.

MIP-1 β concentration tested (500 nM). Clone CCR5-c3 and 3CysA-c1 selected for similar expression levels responded equally to MIP-1 β (Table II). This response was blocked by preincubation with pertussis toxin (PTX) (Fig. 6C).

The forskolin-stimulated cAMP levels were similar in CCR5-c3 and 3CysA-c1 cell lines (cAMP level of 57 ± 12 and 50 ± 9 pmol, respectively), and MIP-1 β caused a dose-dependent inhibition of cAMP accumulation with similar potencies and efficacies (EC_{50} of 3.98 and 3.38 nM, respectively) (Fig. 6D and Table II). This response was totally inhibited by PTX. The functional response of the cell lines were also tested in a microphysiometer, an assay that measures modifications of cell metabolism as the end point of the activation of various intracellular cascades. Typically, the metabolic response of the CCR5-c3 line to 100 nM MIP-1 β is characterized by a biphasic pattern with a transient peak occurring within 2 min following addition of the agonist and a second and longer peak going back to base line after about 20 min. In contrast, the 3CysA-c1 line exhibited only an initial, sharp response and returned to base line much more rapidly (Fig. 6E). When cells were repeatedly stimulated (for 2 min every 10 min) with 100 nM MIP-1 β , the functional response of the 3CysA mutant and wtCCR5 desensitized progressively and in a similar manner (data not shown). We also compared the ability of wtCCR5 and the 3CysA mutant to promote [35 S]GTP γ S binding to membranes prepared from the same clonal cell lines. No difference was seen in basal levels of bound [35 S]GTP γ S. RANTES induced a dose-dependent increase of [35 S]GTP γ S binding to membranes of wtCCR5-expressing cells, with a maximal response about 400% above basal level at a 30 nM concentration. In contrast, a milder response (less than 50% of that for wtCCR5) was obtained with membranes from 3CysA-c1 cells (Fig. 6F). This difference persisted when twice as much 3CysA-c1 membranes were used in the assay (data not shown). These results suggested that palmitoylation of CCR5 contributes to the signaling efficiency of the receptor by allowing its trafficking to the plasma membrane but also that the 3CysA mutant might activate some signaling pathways less efficiently than wtCCR5.

CCR5 Palmitoylation Does Not Influence Chemokine-induced Endocytosis—Cells were incubated, for 45 min at 37 °C, with different concentrations of RANTES or AOP-RANTES and then assayed for surface expression by FACS analysis using the MC-5 mAb. RANTES and AOP-RANTES (although with a greater potency) induced a similar dose-dependent reduction of surface expression of the receptor in CCR5-c3 and 3CysA-c1 cell lines (Fig. 7, A and B), suggesting that palmitoylation does not influence chemokine-induced CCR5 internalization.

CCR5 Palmitoylation and HIV Coreceptor Function—The

coreceptor function of the 3CysA mutant for viruses pseudotyped with three R5 strains Envs (ADA, BaL, and JRFL) was reduced by about 50% as compared with wtCCR5 (data not shown). As for functional response to chemokines, HIV infection is also strongly influenced by the level of CCR5 expression (33). Therefore, to normalize for differences in receptor expression, we transfected cells with different amounts of the plasmid encoding wtCCR5 and then infected with GFP reporter viruses pseudotyped with the BaL Env. After 2 days post-infection, cells were stained with the PE-conjugated 2D7 mAb and assayed for both surface expression (PE fluorescence) and HIV infection (GFP fluorescence) by FACS analysis. As shown in Fig. 8A, dilution of the wtCCR5 plasmid resulted in a reduction of cell surface expression to a level similar to that obtained for the 3CysA mutant. For similar surface expression levels, there was no significant difference in the coreceptor function of wtCCR5 and the 3CysA mutant (Fig. 8B), suggesting that palmitoylation by itself was not important for HIV coreceptor function.

DISCUSSION

The mechanisms controlling intracellular trafficking of GPCRs play a fundamental role in the regulation of receptor functions. Trafficking of CCR5 to and from the plasma membrane has been shown to affect greatly its chemokine receptor and HIV coreceptor functions (7, 8, 16). The level of CCR5 at the cell surface has been correlated with HIV infectivity both *in vitro* and *in vivo* (33, 34), and ligand-mediated CCR5 internalization plays a prominent role in the inhibition of HIV infection by chemokines (17–19). Palmitoylation is a common post-translational modification of membrane and cytosolic proteins, consisting in the acylation of cysteine side chains by palmitic acid. A number of GPCRs have been shown to be palmitoylated on cysteines located within the intracellular carboxyl-terminal domain of the receptor. By anchoring this domain to the plasma membrane, this post-translational modification tends to create a fourth intracellular loop in these receptors (Fig. 1B). GPCRs belonging to different subfamilies are palmitoylated, and mutagenesis of the palmitoylated cysteines is associated with many, and sometimes opposite, effects on the functional properties of the receptors. These include modifications of receptor trafficking, signal transduction and desensitization processes, that might vary according to the receptor studied (23).

CCR5 exhibits a cluster of 3 cysteine residues in its carboxyl-terminal region, which we found represented the main site of CCR5 palmitoylation.

The integrity of the cysteine cluster was important for the transport of CCR5 to the cell surface. Since no significant difference was seen according to which cysteines were mutated in the single and double mutants, it is likely that all three cysteines can be palmitoylated. By using confocal microscopy, we found that the triple cysteine mutant was synthesized but sequestered largely in the ER or Golgi complex, suggesting that much of the protein was misfolded or retained by some other mechanism. Recently, it has been demonstrated that only a fraction of newly synthesized OP $_1$ opioid receptor exits the ER and reach the cell surface (35), whereas the receptors retained in the ER are transported back to the cytosol, ubiquitinated, and degraded by the 26 S proteasome (36). The overall reduction of fluorescent material in cells stably expressing the 3CysA-GFP mutant, as compared with wtCCR5-GFP-expressing cells (data not shown), suggests that the retention of receptors in intracellular compartments probably leads to its early degradation as well. For several other GPCRs, including the thyrotropin, vasopressin V $_2$, and adenosine A $_1$ receptors (37–40), preventing receptor palmitoylation also leads to decreased receptor expression. The underlying mechanism was not dem-

TABLE I
Expression levels, binding, and functional parameters of CCR5 cysteine mutants

The surface expression of wt and mutant CCR5 in CHO-K1 cells as determined by FACS analysis, using the 2D7 mAb, is represented as the MCF. The binding parameters (pK_i and calculated B_{max}) were derived from competition binding assays using ^{125}I -MIP-1 β as tracer. Functional parameters (pEC_{50} and E_{max}) were derived from dose-response curves in the aequorin assay. The data represent the mean \pm S.E. calculated from three separate experiments. NM, not measurable.

	Expression, MCF (2D7)	Binding		Aequorin assay	
		pK_i	B_{max} (sites/cell)	pEC_{50}	E_{max} (% of wt)
wtCCR5	497	9.21 \pm 0.15	161,000 \pm 80,000	7.71 \pm 0.24	100
C321A	206	9.25 \pm 0.11	108,000 \pm 31,000	7.53 \pm 0.26	51 \pm 10.7
C323A	264	9.49 \pm 0.22	53,500 \pm 14,000	7.71 \pm 0.22	43 \pm 9.8
C324A	292	9.64 \pm 0.42	94,000 \pm 9,800	7.62 \pm 0.38	53 \pm 6.9
C321A/C323A	43	9.57 \pm 0.01	16,200 \pm 1,100	NM	NM
C321A/C324A	32	9.55 \pm 0.01	11,600 \pm 1,100	NM	NM
C323A/C324A	31	9.63 \pm 0.33	11,600 \pm 7,600	NM	NM
3CysA	24	9.70 \pm 0.15	6,900 \pm 3,300	NM	NM

TABLE II
Surface expression and functional parameters in different assays for CHO-K1 cell clones expressing similar level of wtCCR5 or the 3CysA mutant

The surface expression of wtCCR5 and the 3CysA mutant in CHO-K1 cell lines as determined by FACS analysis, using the 2D7 mAb, is represented as the MCF. The functional parameters are represented as pEC_{50} and E_{max} for the different assays used in this study. The E_{max} for the aequorin assay is given as percent of the maximal response of the cell line obtained with 10 μ M ATP, for cAMP accumulation, as percent of the forskolin-stimulated cAMP values, and for GTP γ S binding as percent above the base-line values. The data represent the mean \pm S.E. calculated from three separate experiments. The statistical significance of the differences in B_{max} between wtCCR5 and the mutant were calculated using the Student's *t* test (NS, not significant).

	Expression, MCF (2D7)	Aequorin		cAMP inhibition		GTP γ S binding	
		pEC_{50}	E_{max}	pEC_{50}	E_{max}	pEC_{50}	E_{max}
CCR5-c3	284	7.85 \pm 0.22	68.2 \pm 11.0	8.40 \pm 0.15	83.7 \pm 2.3	8.39 \pm 0.20	471 \pm 14
3CysA-c1	231	7.77 \pm 0.09	58.7 \pm 10.7 (NS)	8.47 \pm 0.35	75.3 \pm 9.7 (NS)	8.50 \pm 0.25	297 \pm 15 ($p = 0.004$)

onstrated, however, except for the A₁ receptor, for which enhanced degradation was indeed shown (40).

We used FRAP to investigate, in living cells, the diffusion of wtCCR5-GFP or the 3CysA-GFP mutant into intracellular compartments. The diffusion parameters for wtCCR5-GFP were similar to those derived previously for the β_2 -adrenergic and the gonadotropin-releasing hormone receptor (27, 41). The diffusion of the 3CysA-GFP mutant was severely affected, suggesting that the mutant is associated with slowly diffusing ER proteins and/or forms large aggregates (42). The fourth intracellular loop or the carboxyl-terminal tail of the receptor might interact with other proteins necessary for efficient CCR5 targeting to the plasma membrane, and the proper folding of these domains might require cysteine palmitoylation. For several GPCRs, such as olfactory receptors in *Caenorhabditis elegans*, opsins, and adrenomedullin receptor, specific chaperones or cargo receptors, necessary for their efficient transport to the cell surface, have been identified (43–48). Alternatively, unpalmitoylated receptors might leave accessible patches of hydrophobic residues, favoring interaction with chaperones or aggregation of the receptor, leading to its degradation (49).

Once CCR5 has reached the cell surface, whether it is palmitoylated or not, extracellular domains of the receptor appeared to be correctly folded, since the different cysteine mutants were recognized by mAbs binding conformational or linear epitopes with the same efficiency, and they bound MIP-1 β with the same affinity. For some GPCRs, such as the β_2 -adrenergic or the endothelin ET_A and ET_B receptors, palmitoylation has been found to affect the signaling properties of the receptor (50–52). Low expression of the double and triple cysteine mutants reduced signaling efficiency in transfected cells. For similar expression levels, however, the 3CysA mutant promoted intracellular calcium release and inhibition of cAMP accumulation as efficiently as wtCCR5. In contrast, the kinetics of the cellular response measured by a microphysiometer was much shorter. Repeated stimulation of the mutant receptor did not uncover a

more rapid desensitization of the cellular response. The different kinetics could result from differential coupling between palmitoylated and unpalmitoylated receptors. Indeed, the microphysiometer integrates the metabolic consequences of many different signaling cascades induced by receptor activation, and different signaling cascades are known to result in different profiles of metabolic activity (53). This modified kinetics, and the lower [^{35}S]GTP γ S binding increment to membranes expressing unpalmitoylated receptor, suggest that the 3CysA mutant does not couple as efficiently to some cascades activated by the wild-type receptor. Mutations in other GPCRs have been shown to affect selectively specific signal transduction pathways without affecting others (23). For example, the absence of palmitoylation in the endothelin A receptor prevents its coupling to G α_q without affecting its ability to stimulate G α_s (51). The carboxyl-terminal tail of CCR5 has been shown to be important for G protein coupling (54). A specific structural organization of the carboxyl-terminal domain of CCR5, dependent on its palmitoylation, might therefore be necessary for the efficient coupling to some G protein subtypes and signaling cascades. For example, it has been shown recently that the fourth intracellular loop of activated rhodopsin interacts directly with G α_t and plays a role in the regulation of the $\beta\gamma$ -subunit binding (55, 56).

Many effectors of GPCR signaling are acylated as well. The α -subunits of G proteins are myristoylated and/or palmitoylated and the γ -subunits are prenylated (57, 58), and these post-translational modifications control the association of functional G protein complexes to the plasma membrane (59, 60). Palmitoylation is required for the localization of some signaling proteins in detergent-resistant subdomains of the membrane (61–64). The presence of CCR5 in these raft microdomains has been described and was proposed to play a role in the organization of front-rear polarity in migrating cells (65). It is thus possible that palmitoylation targets CCR5 to particular membrane microdomains, favoring its interaction with specific sig-

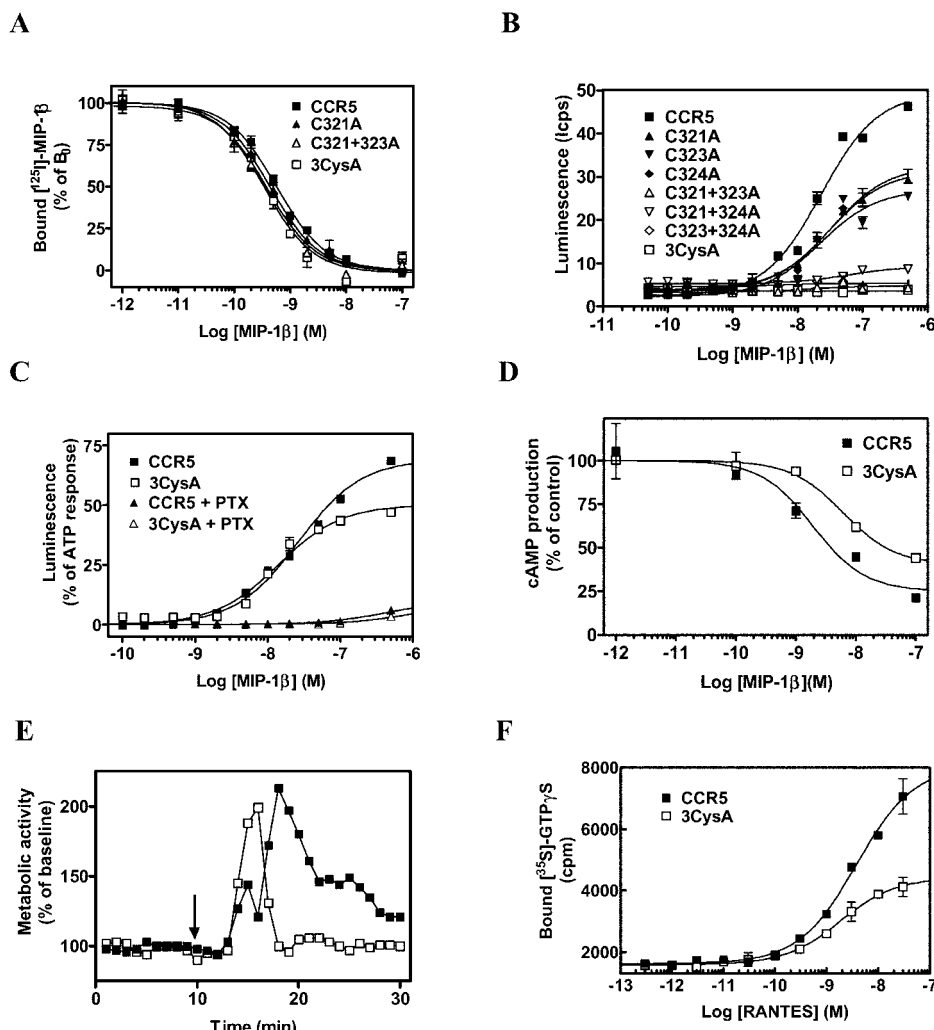


FIG. 6. Binding and functional properties of the cysteine mutants. *A*, competition binding assays were performed on pools of CHO-K1 cells expressing wtCCR5 or the mutants C321A, C321A/C323A and 3CysA, using 0.08 or 0.12 nmol/liter ^{125}I -MIP-1 β as tracer. Results were analyzed by the Graphpad Prism software, using a single-site model, and the data were normalized for nonspecific (0%) and specific binding in the absence of competitor (100%). All points were run in triplicate (error bars, S.E.). Data are representative of three independent experiments. *B*, intracellular calcium release following addition of MIP-1 β was recorded in mixed cell populations coexpressing apoaequorin and the various cysteine mutants. The luminescent signal was recorded for 30 s in a luminometer. Results were analyzed by nonlinear regression. All points were run in triplicate (error bars, S.E.). The displayed curves represent a typical experiment out of three performed independently. *C*, aequorin-based calcium-mobilization assays in response to MIP-1 β were performed on clones expressing similar levels of wtCCR5 (CCR5-c3) or the 3CysA mutant (3CysA-c1), with or without preincubation with PTX (100 ng/ml) for 18 h. All points were run in triplicate (error bars, S.E.). Results were analyzed by non-linear regression, and the data were normalized for basal luminescence (0%) and maximal luminescence obtained by activation of endogenous P_2 receptors by 10 μM ATP (100%). The displayed curves represent a typical experiment out of three performed independently. *D*, inhibition of forskolin-stimulated cAMP accumulation. CCR5-c3 or 3CysA-c1 clones were incubated with 10 μM forskolin and/or MIP-1 β for 15 min, and cAMP was measured by radioimmunoassay. The results were analyzed by nonlinear regression and normalized for basal (0%, in the absence of forskolin) and maximal cAMP levels (100%, in the absence of chemokines). The experiments were performed in duplicate (error bars, S.E.), and the displayed curves represent a typical experiment out of three performed independently. *E*, the metabolic activity of the clones CCR5-c3 (filled squares) and the 3CysA-c1 (open squares) was monitored using a microphysiometer, and the functional response to MIP-1 β (100 nM) was recorded. The results were normalized relative to the basal acidification rates (100%) before addition of the chemokine. Initiation of the stimulation period (2 min) by MIP-1 β is indicated by the arrow. The displayed curves represent a typical experiment out of four performed independently. *F*, effect of RANTES on [^{35}S]GTP γ S binding to membranes from clones CCR5-c3 and 3CysA-c1. Results were analyzed by non-linear regression. The experiments were performed in triplicate (error bars, S.E.), and the displayed curves represent a typical experiment out of two performed independently.

naling proteins, enriched in these membrane subdomains. Further studies will be required to elucidate the role played by rafts in CCR5 (and other GPCRs) signaling.

Chemokine-induced activation of CCR5 promotes the recruitment of G protein-coupled receptor kinases to the plasma membrane, and G protein-coupled receptor kinases mediate the phosphorylation of serine residues in the carboxyl-terminal tail of the receptor, which is followed by receptor endocytosis (20). This mechanism was shown to contribute greatly to the inhibitory effect of chemokines on HIV infection (18). We have shown here that palmitoylation of CCR5 does not seem to affect

receptor internalization (Fig. 8). The role of palmitoylation on GPCR endocytosis varies according to the specific receptor studied. Preventing receptor palmitoylation has been reported to increase (50, 66, 67), decrease (38, 39, 68–70), or not affect (40, 51, 52) internalization of specific GPCRs.

Finally, we have investigated the influence of palmitoylation onto the HIV coreceptor function of CCR5. We found that viral entry was reduced by 50% when the triple cysteine mutant was used as coreceptor. CD4 is also palmitoylated (71), and a constitutive association between CCR5 and CD4 has been demonstrated (72). It has been proposed that membrane raft microdo-

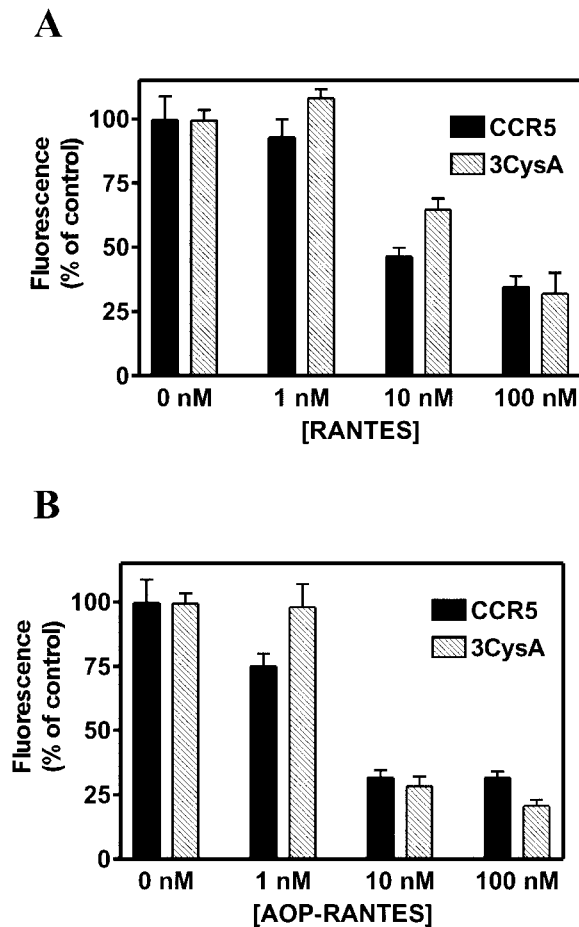


FIG. 7. Chemokine-induced internalization of wtCCR5 and the 3CysA mutant. Internalization of wtCCR5 and the 3CysA mutant, in the presence of RANTES (A) or AOP-RANTES (B), was measured by FACS analysis, using clones CCR5-c1 and 3CysA-c3, and the MC-5 mAb. The cells were incubated for 45 min with different concentrations of chemokines and assayed for surface expression. The data (mean channel fluorescence) were normalized for the autofluorescence of untransfected cells (0%) and the fluorescence obtained in the absence of chemokines (100%). All data points were run in triplicate (error bars, S.E.), and the experiment was performed twice with similar results.

mains play an important role in HIV-1 infection (73), suggesting that absence of palmitoylation might affect coreceptor function (74, 75). However, at comparable levels of binding sites, the coreceptor activity was similar between wtCCR5 and the 3CysA mutant, demonstrating that, when the CD4 concentration is not limiting, palmitoylation of CCR5 is not by itself important for HIV entry.

In conclusion, palmitoylation represents an important post-translational modification influencing greatly the global function of CCR5. The relative conservation of cysteines in the carboxyl-terminal domain of about 80% of GPCRs suggests that palmitoylation likely plays similar structural roles in many receptors. Anchorage of the carboxyl-terminal domain of the receptor to the plasma membrane may secure the correct presentation of the receptor tail. Although the recently described crystal structure of bovine rhodopsin does not include lipids, the position of the side chains of Cys-322 and Cys-323 are consistent with this model (76). As not all GPCRs display cysteines in their carboxyl-terminal domain, palmitoylation is obviously dispensable in some receptors. In this study, we found that for CCR5, disruption of palmitoylation results in a strong reduction of its surface expression in CHO-K1 cells, by alteration of its intracellular trafficking, but also of its ability to interact with so far uncharacterized signaling and/or regu-

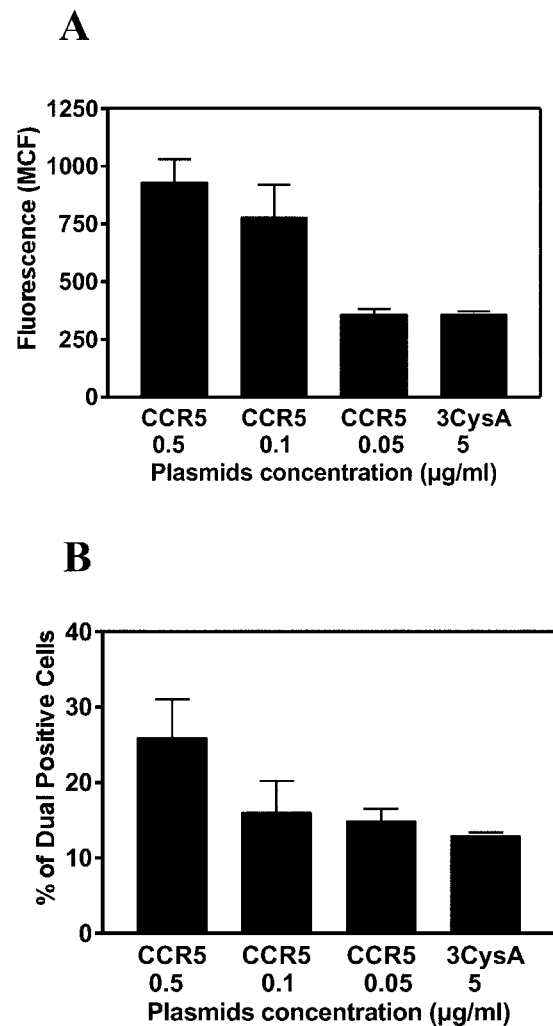


FIG. 8. HIV coreceptor function of wtCCR5 and the 3CysA mutant. 293T cells were transfected with a plasmid encoding wtCCR5 (0.5, 0.1, and 0.05 µg/ml) or the 3CysA mutant (5 µg/ml) together with a plasmid encoding human CD4. The next day, the cells were tested for receptor expression by FACS analysis, using the phycoerythrin-labeled 2D7 mAb (A) or infected with GFP reporter viruses pseudotyped with the R5 tropic Env protein BaL (B). The percentage of dual positive cells (GFP and 2D7-PE) after 2 days is presented. All conditions were performed in duplicate (error bars, S.E.), and the displayed results are representative of two experiments performed independently.

latory proteins. Whether these functions can be generalized to leukocytes in which CCR5 is naturally expressed and to the other members of the chemokine receptor subfamily that are potentially palmitoylated remains to be determined.

Acknowledgments—We thank M. J. Simons, M. E. Decobecq, K. Gillard, and H. Nguyen Tran for expert technical assistance. We thank A. Proudfoot for kindly providing AOP-RANTES, M. Mack for mAbs, D. Communi for running mass spectrometry, and the AIDS Research and Reference Reagent Program for sCD4.

REFERENCES

- Samson, M., Labbe, O., Mollereau, C., Vassart, G., and Parmentier, M. (1996) *Biochemistry* **35**, 3362–3367
- Gong, W., Howard, O. M., Turpin, J. A., Grimm, M. C., Ueda, H., Gray, P. W., Raport, C. J., Oppenheim, J. J., and Wang, J. M. (1998) *J. Biol. Chem.* **273**, 4289–4292
- Nibbs, R. J., Yang, J., Landau, N. R., Mao, J. H., and Graham, G. J. (1999) *J. Biol. Chem.* **274**, 17478–17483
- Detheux, M., Standker, L., Vakili, J., Munch, J., Forssmann, U., Adermann, K., Pohlmann, S., Vassart, G., Kirchhoff, F., Parmentier, M., and Forssmann, W. G. (2000) *J. Exp. Med.* **192**, 1501–1508
- Littman, D. R. (1998) *Cell* **93**, 677–680
- Berger, E. A., Murphy, P. M., and Farber, J. M. (1999) *Annu. Rev. Immunol.* **17**, 657–700
- Samson, M., Libert, F., Doranz, B. J., Rucker, J., Liesnard, C., Farber, C. M.,

- Saragosti, S., Lapoumeroulie, C., Cognaux, J., Forceille, C., Muyldermans, G., Verhofstede, C., Burtonboy, G., Georges, M., Imai, T., Rana, S., Yi, Y., Smyth, R. J., Collman, R. G., Doms, R. W., Vassart, G., and Parmentier, M. (1996) *Nature* **382**, 722–725
8. Liu, R., Paxton, W. A., Choe, S., Ceradini, D., Martin, S. R., Horuk, R., MacDonald, M. E., Stuhlmann, H., Koup, R. A., and Landau, N. R. (1996) *Cell* **86**, 367–377
 9. Garred, P., Madsen, H. O., Petersen, J., Marquart, H., Hansen, T. M., Freiesleben, S. S., Volck, B., Svejgaard, A., and Andersen, V. (1998) *J. Rheumatol.* **25**, 1462–1465
 10. Qin, S., Rottman, J. B., Myers, P., Kassam, N., Weinblatt, M., Loetscher, M., Koch, A. E., Moser, B., and Mackay, C. R. (1998) *J. Clin. Invest.* **101**, 746–754
 11. Mack, M., Bruhl, H., Gruber, R., Jaeger, C., Cihak, J., Eiter, V., Plachy, J., Stangassinger, M., Uhlig, K., Schattenkirchner, M., and Schlondorff, D. (1999) *Arthritis & Rheum.* **42**, 981–988
 12. Balashov, K. E., Rottman, J. B., Weiner, H. L., and Hancock, W. W. (1999) *Proc. Natl. Acad. Sci. U. S. A.* **96**, 6873–6878
 13. Hall, I. P., Wheatley, A., Christie, G., McDougall, C., Hubbard, R., and Helms, P. J. (1999) *Lancet* **354**, 1264–1265
 14. Carroll, R. G., Riley, J. L., Levine, B. L., Feng, Y., Kaushal, S., Ritchey, D. W., Bernstein, W., Weislow, O. S., Brown, C. R., Berger, E. A., June, C. H., and St. Louis, D. C. (1997) *Science* **276**, 273–276
 15. Rana, S., Besson, G., Cook, D. G., Rucker, J., Smyth, R. J., Yi, Y., Turner, J. D., Guo, H. H., Du, J. G., Peiper, S. C., Lavi, E., Samson, M., Libert, F., Liesnard, C., Vassart, G., Doms, R. W., Parmentier, M., and Collman, R. G. (1997) *J. Virol.* **71**, 3219–3227
 16. Blanpain, C., Lee, B., Tackoen, M., Puffer, B., Boom, A., Libert, F., Sharron, M., Wittamer, V., Vassart, G., Doms, R. W., and Parmentier, M. (2000) *Blood* **96**, 1638–1645
 17. Alkhatib, G., Locati, M., Kennedy, P. E., Murphy, P. M., and Berger, E. A. (1997) *Virology* **234**, 340–348
 18. Mack, M., Luckow, B., Nelson, P. J., Cihak, J., Simmons, G., Clapham, P. R., Signoret, N., Marsh, M., Stangassinger, M., Borlat, F., Wells, T. N., Schlondorff, D., and Proudfoot, A. E. (1998) *J. Exp. Med.* **187**, 1215–1224
 19. Blanpain, C., Migeotte, I., Lee, B., Vakili, J., Doranz, B. J., Govaerts, C., Vassart, G., Doms, R. W., and Parmentier, M. (1999) *Blood* **94**, 1899–1905
 20. Oppermann, M., Mack, M., Proudfoot, A. E., and Olbrich, H. (1999) *J. Biol. Chem.* **274**, 8875–8885
 21. Blanpain, C., Lee, B., Vakili, J., Doranz, B. J., Govaerts, C., Migeotte, I., Sharron, M., Dupriez, V., Vassart, G., Doms, R. W., and Parmentier, M. (1999) *J. Biol. Chem.* **274**, 18902–18908
 22. Farzan, M., Mirzabekov, T., Kolchinsky, P., Wyatt, R., Cayabyab, M., Gerard, N. P., Gerard, C., Sodroski, J., and Choe, H. (1999) *Cell* **96**, 667–676
 23. Morello, J. P., and Bouvier, M. (1996) *Biochem. Cell Biol.* **74**, 449–457
 24. Samson, M., LaRosa, G., Libert, F., Painsdavoine, P., Dethoux, M., Vassart, G., and Parmentier, M. (1997) *J. Biol. Chem.* **272**, 24934–24941
 25. Takebe, Y., Seiki, M., Fujisawa, J., Hoy, P., Yokota, K., Arai, K., Yoshida, M., and Arai, N. (1988) *Mol. Cell. Biol.* **8**, 466–472
 26. Mirzabekov, T., Bannert, N., Farzan, M., Hofmann, W., Kolchinsky, P., Wu, L., Wyatt, R., and Sodroski, J. (1999) *J. Biol. Chem.* **274**, 28745–28750
 27. Barak, L. S., Ferguson, S. S., Zhang, J., Martenson, C., Meyer, T., and Caron, M. G. (1997) *Mol. Pharmacol.* **51**, 177–184
 28. Stables, J., Green, A., Marshall, F., Fraser, N., Knight, E., Sautel, M., Milligan, G., Lee, M., and Rees, S. (1997) *Anal. Biochem.* **252**, 115–126
 29. Connor, R. I., Chen, B. K., Choe, S., and Landau, N. R. (1995) *Virology* **206**, 935–944
 30. Lee, B., Sharron, M., Blanpain, C., Doranz, B. J., Vakili, J., Setoh, P., Berg, E., Liu, G., Guy, H. R., Durell, S. R., Parmentier, M., Chang, C. N., Price, K., Tsang, M., and Doms, R. W. (1999) *J. Biol. Chem.* **274**, 9617–9626
 31. Pfanner, N., Orci, L., Glick, B. S., Amherdt, M., Arden, S. R., Malhotra, V., and Rothman, J. E. (1989) *Cell* **59**, 95–102
 32. Axelrod, D., Ravdin, P., Koppel, D. E., Schlessinger, J., Webb, W. W., Elson, E. L., and Podleski, T. R. (1976) *Proc. Natl. Acad. Sci. U. S. A.* **73**, 4594–4598
 33. Wu, L., Paxton, W. A., Kassam, N., Ruffing, N., Rottman, J. B., Sullivan, N., Choe, H., Sodroski, J., Newman, W., Koup, R. A., and Mackay, C. R. (1997) *J. Exp. Med.* **185**, 1681–1691
 34. Reynes, J., Portales, P., Segondy, M., Baillat, V., Andre, P., Reant, B., Avinens, O., Couderc, G., Benkirane, M., Clot, J., Eliaou, J. F., and Corbeau, P. (2000) *J. Infect. Dis.* **181**, 927–932
 35. Petaja-Repo, U. E., Hogue, M., Laperriere, A., Walker, P., and Bouvier, M. (2000) *J. Biol. Chem.* **275**, 13727–13736
 36. Petaja-Repo, U. E., Hogue, M., Laperriere, A., Bhalla, S., Walker, P., and Bouvier, M. (2001) *J. Biol. Chem.* **276**, 4416–4423
 37. Tanaka, K., Nagayama, Y., Nishihara, E., Namba, H., Yamashita, S., and Niwa, M. (1998) *Endocrinology* **139**, 803–806
 38. Schulein, R., Liebenhoff, U., Muller, H., Birnbaumer, M., and Rosenthal, W. (1996) *Biochem. J.* **313**, 611–616
 39. Sadeghi, H. M., Innamorati, G., Dagarag, M., and Birnbaumer, M. (1997) *Mol. Pharmacol.* **52**, 21–29
 40. Gao, Z., Ni, Y., Szabo, G., and Linden, J. (1999) *Biochem. J.* **342**, 387–395
 41. Nelson, S., Horvat, R. D., Malvey, J., Roess, D. A., Barisas, B. G., and Clay, C. M. (1999) *Endocrinology* **140**, 950–957
 42. Nehls, S., Snapp, E. L., Cole, N. B., Zaal, K. J., Kenworthy, A. K., Roberts, T. H., Ellenberg, J., Presley, J. F., Siggia, E., and Lippincott-Schwartz, J. (2000) *Nat. Cell Biol.* **2**, 288–295
 43. Dwyer, N. D., Troemel, E. R., Sengupta, P., and Bargmann, C. I. (1998) *Cell* **93**, 455–466
 44. Gimelbrant, A. A., Haley, S. L., and McClintock, T. S. (2001) *J. Biol. Chem.* **276**, 7285–7290
 45. Baker, E. K., Colley, N. J., and Zuker, C. S. (1994) *EMBO J.* **13**, 4886–4895
 46. Yeung, D. E., Brown, G. W., Tam, P., Russnak, R. H., Wilson, G., Clark-Lewis, I., and Astell, C. R. (1991) *Virology* **181**, 35–45
 47. Tai, A. W., Chuang, J. Z., Bode, C., Wolfmum, U., and Sung, C. H. (1999) *Cell* **97**, 877–887
 48. McLatchie, L. M., Fraser, N. J., Main, M. J., Wise, A., Brown, J., Thompson, N., Solari, R., Lee, M. G., and Foord, S. M. (1998) *Nature* **393**, 333–339
 49. Wickner, S., Maurizi, M. R., and Gottesman, S. (1999) *Science* **286**, 1888–1893
 50. Moffett, S., Mouillac, B., Bonin, H., and Bouvier, M. (1993) *EMBO J.* **12**, 349–356
 51. Horstmeyer, A., Cramer, H., Sauer, T., Muller-Esterl, W., and Schroeder, C. (1996) *J. Biol. Chem.* **271**, 20811–20819
 52. Okamoto, Y., Ninomiya, H., Tanioka, M., Sakamoto, A., Miwa, S., and Masaki, T. (1997) *J. Biol. Chem.* **272**, 21589–21596
 53. Owicki, J. C., Parce, J. W., Kercso, K. M., Sigal, G. B., Muir, V. C., Venter, J. C., Fraser, C. M., and McConnell, H. M. (1990) *Proc. Natl. Acad. Sci. U. S. A.* **87**, 4007–4011
 54. Gosling, J., Monteclaro, F. S., Atchison, R. E., Arai, H., Tsou, C. L., Goldsmith, M. A., and Charo, I. F. (1997) *Proc. Natl. Acad. Sci. U. S. A.* **94**, 5061–5066
 55. Marin, E. P., Krishna, A. G., Zvyaga, T. A., Isele, J., Siebert, F., and Sakmar, T. P. (2000) *J. Biol. Chem.* **275**, 1930–1936
 56. Ernst, O. P., Meyer, C. K., Marin, E. P., Henklein, P., Fu, W. Y., Sakmar, T. P., and Hofmann, K. P. (2000) *J. Biol. Chem.* **275**, 1937–1943
 57. Wedegaertner, P. B., Wilson, P. T., and Bourne, H. R. (1995) *J. Biol. Chem.* **270**, 503–506
 58. Casey, P. J. (1995) *Science* **268**, 221–225
 59. Fishburn, C. S., Herzmark, P., Morales, J., and Bourne, H. R. (1999) *J. Biol. Chem.* **274**, 18793–18800
 60. Evanko, D. S., Thiagarajan, M. M., and Wedegaertner, P. B. (2000) *J. Biol. Chem.* **275**, 1327–1336
 61. Moffett, S., Brown, D. A., and Linder, M. E. (2000) *J. Biol. Chem.* **275**, 2191–2198
 62. Arni, S., Keilbaugh, S. A., Ostermeyer, A. G., and Brown, D. A. (1998) *J. Biol. Chem.* **273**, 28478–28485
 63. Zhang, W., Tribble, R. P., and Samelson, L. E. (1998) *Immunity* **9**, 239–246
 64. Melkonian, K. A., Ostermeyer, A. G., Chen, J. Z., Roth, M. G., and Brown, D. A. (1999) *J. Biol. Chem.* **274**, 3910–3917
 65. Manes, S., Mira, E., Gomez-Mouton, C., Lacalle, R. A., Keller, P., Labrador, J. P., and Martinez, A. (1999) *EMBO J.* **18**, 6211–6220
 66. Moffett, S., Adam, L., Bonin, H., Loisel, T. P., Bouvier, M., and Mouillac, B. (1996) *J. Biol. Chem.* **271**, 21490–21497
 67. Kawate, N., Peegel, H., and Menon, K. M. (1997) *Mol. Cell. Endocrinol.* **127**, 211–219
 68. Kosugi, S., and Mori, T. (1996) *Biochem. Biophys. Res. Commun.* **221**, 636–640
 69. Eason, M. G., Jacinto, M. T., Theiss, C. T., and Liggett, S. B. (1994) *Proc. Natl. Acad. Sci. U. S. A.* **91**, 11178–11182
 70. Faussner, A., Proud, D., Towns, M., and Bathon, J. M. (1998) *J. Biol. Chem.* **273**, 2617–2623
 71. Crise, B., and Rose, J. K. (1992) *J. Biol. Chem.* **267**, 13593–13597
 72. Xiao, X., Wu, L., Stantchev, T. S., Feng, Y. R., Ugolini, S., Chen, H., Shen, Z., Riley, J. L., Broder, C. C., Sattentau, Q. J., and Dimitrov, D. S. (1999) *Proc. Natl. Acad. Sci. U. S. A.* **96**, 7496–7501
 73. Manes, S., del Real, G., Lacalle, R. A., Gomez-Mouton, C., Sanchez-Palomino, S., Delgado, R., Alcami, J., Mira, E., and Martinez-A, C. (2000) *EMBO Reports* **1**, 190–196
 74. Nguyen, D. H., and Hildreth, J. E. (2000) *J. Virol.* **74**, 3264–3272
 75. Hug, P., Lin, H. M., Korte, T., Xiao, X., Dimitrov, D. S., Wang, J. M., Puri, A., and Blumenthal, R. (2000) *J. Virol.* **74**, 6377–6385
 76. Palczewski, K., Kumasaka, T., Hori, T., Behnke, C. A., Motoshima, H., Fox, B. A., Le, T., I. Teller, D. C., Okada, T., Stenkamp, R. E., Yamamoto, M., and Miyano, M. (2000) *Science* **289**, 739–745